Rock and Soil Mechanics

Volume 44 | Issue 1 Article 1

3-13-2023

Shear damage mechanism of coarse-grained materials considering strain localization

Shun-li ZHAO
Yellow River Engineering Consulting Co., Ltd., Zhengzhou, Henan 450003, China

Zhi-jun YANG
School of Civil Engineering, Wuhan University, Wuhan, Hubei 430072, China

Xu-dong FU
School of Civil Engineering, Wuhan University, Wuhan, Hubei 430072, China

Zheng FANG
School of Civil Engineering, Wuhan University, Wuhan, Hubei 430072, China, zfang@whu.edu.cn

Rock and Soil Mechanics 2023 44(1): 31−42 ISSN 1000−7598
https: //doi.org/10.16285/j.rsm.2022.5221 rocksoilmech.researchcommons.org/journal

Shear damage mechanism of coarse-grained materials considering strain localization

ZHAO Shun-li[1, 2], YANG Zhi-jun[1], FU Xu-dong[1], FANG Zheng[1]

1. School of Civil Engineering, Wuhan University, Wuhan, Hubei 430072, China
2. Yellow River Engineering Consulting Co., Ltd., Zhengzhou, Henan 450003, China

Abstract: In view of the mechanical properties of coarse-grained materials, such as strain softening and dilatancy, a generalized shear damage mechanical model with wide applicability was established in this study by considering the strain localization phenomenon marked by shear band. This damage model adopted the mathematical simplification of shear band in the envelope theory, and the stress-strain relationship equation of coarse-grained material was derived based on the strain equivalence principle and Weibull distribution. A nonlinear functional relationship between axial and volumetric plastic strain was proposed to describe the weakening of dilatancy based on the mechanism of dilatancy. Combined with the servo process of coarse-grained materials in triaxial compression tests, a method to determine the parameters of damage model was proposed based on genetic algorithm. By conducting a series of triaxial compression tests under different confining pressures, the shear damage mechanical model was validated, and the effects of the evolution of shear band parameters on the strength and deformation characteristics of coarse-grained materials were further analyzed. The results indicate that the proposed shear damage mechanical model considering the strain localization characteristics can accurately simulate the strain-softening and dilatancy characteristics of coarse-grained materials, and effectively reveal the influence mechanism of the internal deformation of the shear band on the overall macroscopic deformation of the coarse-grained sample. The evolution of the shear band parameters with the surrounding confining pressures in the model was consistent with the mesoscopic mechanism of coarse-grained materials. The strength composition calculated by this model was in good agreement with the micro mechanism, such as the breakage and reorganization of coarse-grained particles.

Keywords: coarse-grained material; shear damage; stress-strain equation; strain localization; strain softening; dilatancy

1 Introduction

Coarse-grained materials have prominent advantages such as high shear strength, good compaction characteristics and small settlement deformation, so they are widely used in earth-rock dam, subgrade filling and other projects[1−2]. The mechanical properties of coarse-grained materials are greatly affected by particle gradation, bulk density and internal structure. Therefore, coarse-grained materials can exhibit obvious strain softening or strain hardening characteristics, and dilatancy is obvious for them at low confining pressure[3]. Through discrete element numerical simulation, Gu et al. [4] pointed out that the causes of dilatancy of granular materials are closely related to the occurrence of shear bands. Both test results and theoretical analysis show that the strain localization characteristic of coarse-grained materials marked by shear band is the key factor affecting the mechanical characteristics of coarse-grained materials [5−7].

Some classical constitutive models of soil mechanics, such as Mohr-Coulomb model, Duncan-Chang model, and Cambridge model, have the problem of failing to express the mechanical mechanism of strain softening. Therefore, one of the focuses of current research is to construct a mechanical model with wide applicability that can reflect the deformation and failure characteristics of coarse-grained materials from the point of view of the internal structure of coarse-grained materials. The existing research on the deformation characteristics of coarse-grained materials is mainly carried out under the framework of elastic-plastic theory. For example, Liu et al.[1] derived a constitutive model of coarse-grained materials based on the distribution of contact forces and contact points at different contact angles between particles, but they did not consider the crushing characteristics of coarse particles, so their constitutive model could not characterize the strain softening characteristics. Some studies have shown that the strain softening characteristics of coarse-grained materials during shear failure can be well simulated by taking into account the effect of particle breakage in the shear failure process and the corresponding nonlinear critical state line[8−9]. However, due to insufficient consideration of strain localization characteristics, the meso-mechanism of coarse-grained materials cannot be further reflected.

The particle breakage occurring in the shear failure process of coarse-grained materials can be considered as a damage process. By setting the corresponding damage variable D, the gradualistic characteristics of

Received: 28 February 2022 Accepted: 17 September 2022
This work was supported by the National Natural Science Foundation of China (51978540).
First author: ZHAO Shun-li, male, born in 1992, PhD candidate, mainly engaged in geotechnical investigation and testing and constitutive model development. E-mail: slzhao@whu.edu.cn
Corresponding author: FANG Zheng, male, born in 1966, PhD, Professor, Doctoral supervisor, research interests: theory of disaster mitigation and prevention systems in civil engineering. E-mail: zfang@whu.edu.cn

strain softening can be well simulated. For example, Hou et al.[10] built a creep model suitable for coarse-grained materials at the frozen state based on damage theory, and Ling et al.[11] further derived the damage mechanics model considering the freeze-thaw cycles. Nowadays, the existing research believes that the damage process the existing studies consider that the damage process acts on the whole specimen when constructing the damage model. However, when the damage variable D=1, that is, the sample reaches complete damage, the theoretical results and the actual situation have obvious contradictions. For example, if damage is defined by strength, the residual strength will be equal to 0. If damage is defined by elastic modulus, the increasing trend of initial elastic modulus of soil under cyclic load cannot be explained. More importantly, the strain localization characteristics of shear band cannot be reflected when coarse-grained materials are damaged.

Tejchman et al.[5] pointed out that strain localization, as an essential characteristic of deformation and failure of coarse-grained materials, should be reflected in the construction of relevant models. In view of the phenomenon of strain localization of rock, Brady[12] put forward the inclusion theory, where the shear band is regarded as a low-elastic material, and the damage is mainly concentrated in the shear band, while the area outside the shear band is regarded as a high-elastic material, and He further analyzed the rationality of this mathematical simplification. Liu et al.[13] also suggested use of the inclusion theory for the constitutive model construct to address the strain localization at the strain softening stage, but did not propose a specific constitutive model. In fact, for coarse-grained materials, strong particle breakage and particle reorganization mainly occur in the shear band [5, 14]. The test results also show that, after reaching the strength peak, the deformation inside the shear band is much larger than that in other areas [15], so the shear band of coarse-grained materials can be mathematically simplified according to the inclusion theory.

In order to solve the problem of insufficient consideration of strain localization in the study of mechanical mechanisms of coarse grained materials, in this study, by combining the deformation and failure characteristics of coarse-grained materials and the corresponding gradualistic damage process, a shear damage mechanical model considering strain localization is constructed, and the stress−strain relationship is derived based on the assumption of inclusion theory. The applicability of the damage mechanics model proposed in this study is verified by the actual test data. From the mesoscopic point of view, based on the strength composition of coarse-grained materials, the influence of the evolution of the parameters of the damage mechanics model on the stress-strain curve is further analyzed. Finally, the influence mechanism of the deformation inside the shear band on the overall macroscopic deformation of the sample is revealed.

2 Shear damage mechanics model

2.1 Deformation and failure characteristics

Under triaxial compression, the typical stress−strain relationship curve of coarse-grained materials is shown in Fig.1[1], presenting obvious strain softening and dilatancy characteristics. It can be seen that the dilatancy point usually begins to appear before the peak strength, and with the continuous increase of strain, the dilatancy will weaken and eventually reach a state of no dilatancy. In the case of high content of coarse particles and low confining pressure, the characteristics of strain softening and dilatancy are more obvious [2].

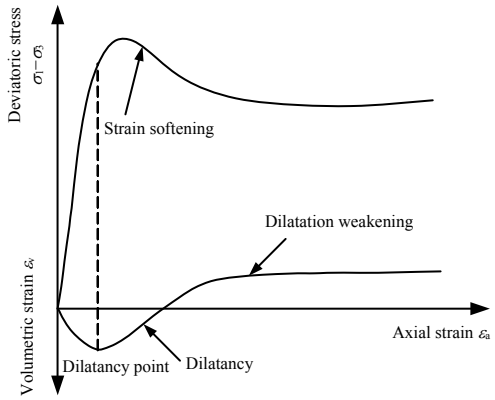

Fig. 1 Typical stress−strain curves of coarse-grained material[1]

In view of the dilatancy of granular materials, Rowe [16] took the sandy soil as the research object and proposed the zigzag shear plane failure mode shown in Fig.2 based on the minimum energy criterion between particles, which has been widely applied in the interpretation of dilatancy mechanism of coarse-grained materials[17]. For granular materials such as coarse-grained materials, the fluctuation of the actual shear plane is the essential cause of dilatancy.

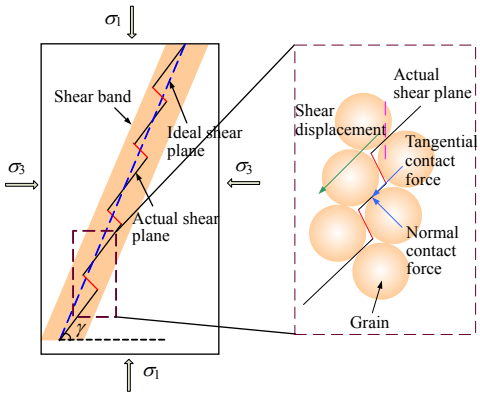

Fig. 2 Schematic diagram of dilatancy principle inside granular material [16]

In addition to strain-softening type stress−strain curve, coarse-grained materials also exhibit strain hardening characteristics under the conditions of high confining pressure, high fines content, and low compactness. Therefore, while revealing the stress−strain characteristics of strain softening and strain hardening, the mechanical model of coarse-grained materials should further consider the nature of the shear band and the characteristic of dilatancy.

2.2 Strain inside the shear band

If the coarse-grained material itself is regarded as an aggregate composed of different micro-units, the damage characteristics of coarse-grained material are closely related to the bearing capacity of these internal structural micro-units. After the strength loss of micro-units, the bearing capacity will be significantly reduced. For coarse-grained materials, due to the interlock force of internal particles, the coarse-grained materials will still show certain cohesion in the process of shear damage, which is also called apparent cohesion. The process of particle breakage inside the shear band can be regarded as the process of loss of cohesion, i.e., the process of damage.

We take the specimen in the conventional triaxial compression test as the research object, equate the dilatancy characteristics in Fig. 2 with the shear damage model in Fig. 3 in term of the inclusion theory. The shear band is mathematically simplified according to the inclusion theory, and it is considered that the shear band after damage is an inclusion with a low- elastic modulus in the overall high-elastic modulus material, that is, the shear damage mainly occurs inside the shear band, which is also supported by previous theories and experimental studies [5,14−15]. By using finite element method, Brady [12] verified that such ideal mathematical simplification would not have a significant effect on the stress field characteristics in and around the inclusion.

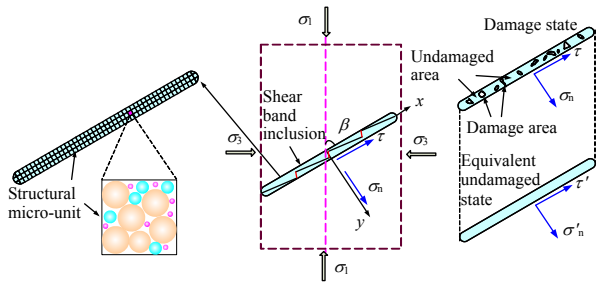

(a) Shear band micro-unit (b) Undamaged state (c) Equivalence principle of strain

Fig. 3 Shear damage model

According to the basic principle of elasticity, the stress state of shear band inclusion in undamaged state is shown as follows:

$$\left.\begin{aligned}\sigma_{\mathrm{n}} &= \sigma_1 \sin^2\beta + \sigma_3 \cos^2\beta \\ \tau &= (\sigma_1 - \sigma_3)\sin\beta\cos\beta\end{aligned}\right\} \tag{1}$$

where σ_{n} is the normal stress on the shear band inclusion; τ is the tangential stress on the shear band inclusion; σ_1 and σ_3 are the maximum and minimum principal stresses, respectively; and β is the angle between the shear band inclusion and the maximum principal stress.

The shear stress on the shear plane is partly contributed by the friction between particles and partly by the interlock force between particles. The loss of interlock force is the essence of the shear failure of coarse-grained materials. Therefore, this paper focuses on analyzing the change of shear stress contributed by interlock force and the corresponding damage. The shear stress contributed by the interlock force $\Delta\tau$, can be calculated as follows:

$$\Delta\tau = \begin{cases}\tau - f\sigma_{\mathrm{n}}, & \tau > f\sigma_{\mathrm{n}} \\ 0, & \tau \leqslant f\sigma_{\mathrm{n}}\end{cases} \tag{2}$$

where f is the friction coefficient.

According to the elastic theory, the shear displacement of the shear band inclusion along the tangential stress direction can be expressed by the following equation:

$$u = \frac{\Delta\tau}{k_{\mathrm{s}}} \tag{3}$$

where u is shear displacement and k_{s} is the shear stiffness. The shear stiffness is mainly related to the shear slip of the particles inside the shear band inclusion.

The shear displacement (u) generated by the shear band inclusion in the direction of the maximum principal stress forms a strain that can be derived from the following equation:

$$\varepsilon_\tau = H\frac{\Delta\tau\cos\beta}{k_{\mathrm{s}}} \tag{4}$$

where ε_τ is the axial strain in the direction of maximum principal stress formed by shear displacement; H is the proportion coefficient, which is the proportion of shear band inclusion to the total volume of the sample.

2.3 Stress−strain equation

When there is no damage to the shear band inclusion, the stress−strain relationship of the specimen can be calculated by Hooke's law, and the strain calculated by Eq.(4) is still part of the elastic deformation. With the increase of deviatoric stress, when the shear band inclusion is locally damaged, the damaged part can be considered to be in a plastic flow state, and its bearing capacity degrades to the residual friction strength. The damage variable D defined by damage area can be calculated as follow:

$$D = 1 - A'/A \tag{5}$$

where A is the loaded area before the shear band damage. When the shear band is damaged, A' is the undamaged area. As shown in Fig.3, according to the equivalent principle of strain applied to shear band

inclusion[18], the following relationship can be obtained:

$$\varepsilon_\tau = H\frac{\Delta\tau\cos\beta}{k_s'} = H\frac{\Delta\tau'\cos\beta}{k_s} \tag{6}$$

$$\tau A = \tau' A' + (A - A')f\sigma_n \tag{7}$$

where k_s' is the equivalent shear stiffness of the shear inclusion in the damaged state; τ' is the nominal shear stress in the equivalent undamaged state; and $\Delta\tau'$ is the nominal shear stress contributed by the interlock force in the equivalent undamaged state.

The calculation equation of damage variable D expressed by shear stiffness can be obtained by combining Eqs. (5) to (7) as follows:

$$k_s' = k_s(1 - D) \tag{8}$$

The undamaged part of the shear band inclusion bears the shear force exceeding the friction strength, which can be expressed by the following equation:

$$c_F = \frac{\Delta\tau A}{A'} = \frac{\Delta\tau}{1 - D} \tag{9}$$

where c_F is the shear stress contributed by the interlock force of the undamaged part.

The macro-mechanical properties of coarse-grained materials are controlled by the microstructure. It is assumed that the cohesion of the micro-unit c inside the shear band of coarse-grained material follows the probability distribution in the whole space of the shear band. With the continuous increase of shear stress, when the cohesion of the micro-unit c is less than c_F, the micro-unit will be damaged. Studies have shown that the Weibull distribution can be used to quantitatively describe the distribution characteristics of the cohesion of soil micro-units [8–9, 19]:

$$\phi(c) = \frac{m}{C_0}\left(\frac{c}{C_0}\right)^{m-1} \mathrm{e}^{-(\frac{c}{C_0})^m} = \frac{\mathrm{d}D}{\mathrm{d}c} \tag{10}$$

where $\phi(c)$ is the probability density function of the cohesion of soil micro-units; both C_0 and m are parameters of Weibull distribution; and c is the cohesion of the micro-unit.

By integrating Eq.(10), the relationship between the damage variable D of the loaded damage and the cohesion of soil micro-units c is

$$D = 1 - \exp\left[-\left(\frac{c}{C_0}\right)^m\right] \tag{11}$$

The axial strain of coarse-grained materials ε_a can be divided into two parts, namely, elastic strain ε_a^e and plastic strain ε_a^p.

$$\varepsilon_a = \varepsilon_a^e + \varepsilon_a^p \tag{12}$$

ε_a^e can be calculated by the following equation:

$$\varepsilon_a^e = (\sigma_1 - \sigma_3)/E \tag{13}$$

where E is the initial elastic modulus of coarse-grained materials.

ε_a^p is the plastic strain induced by the shear damage of shear band inclusion, i.e,

$$\varepsilon_a^p = \frac{\Delta\tau H\cos\beta}{L_0}\left(\frac{1}{k_s'} - \frac{1}{k_s}\right) \tag{14}$$

where L_0 is the axial height of the coarse-grained specimen.

By substituting Eq. (8) into Eq.(14), we can get

$$\varepsilon_a^p = H\cos\beta\frac{\Delta\tau D}{L_0 k_s(1 - D)} \tag{15}$$

By combining Eqs. (9)−(15), the stress−strain relationship applicable to coarse-grained materials can be obtained as follows:

$$\left.\begin{aligned}
&\varepsilon_a = TK\left\{\frac{1}{\exp\left[-\left(\dfrac{c}{C_0}\right)^m\right]} - 1\right\} + \frac{\sigma_1 - \sigma_3}{E}\\
&c = \frac{(\varepsilon_a - \varepsilon_a^e)}{K} + T\\
&T = (\sigma_1 - \sigma_3)\sin\beta\cos\beta - f(\sigma_1\sin^2\beta + \sigma_3\cos^2\beta)\\
&K = H\cos\beta/(L_0 k_s)
\end{aligned}\right\} \tag{16}$$

By constructing the shear damage model, the stress−strain relationship considering the strain localization characteristics is derived. In practical application, the damage outside the shear band can also be equivalent to a part of the shear band inclusion. According to the above derivation, this equivalence does not affect the final form of Eq.(16). From a model building perspective, this equivalence is also reasonable.

Different from the traditional overall damage, the damage during shear mainly refers to the process of reducing the bearing capacity to the frictional strength due to the particle breakage and particle reorganization inside the shear band. The damage parameter is mainly defined by the ratio of the number of damaged structural micro-units inside the shear band to the original structural micro-units. The particle distribution inside the coarse-grained material can be regarded as the overall uniform distribution. Therefore, the relationship between the damage mechanics of the continuum and the tiny particle aggregate represented by the idealized micro-units is established, and the stress−strain relationship applicable to the coarse-grained material is derived. The stress−strain relationship presented in Eq.(16) is a manifestation of the overall macroscopic mechanical mechanism of the coarse-grained material sample based on the shear band damage on a microscopic scale.

2.4 Volumetric strain equation

As the damage model established by strain equivalence principle mainly considers the relationship between axial strain and stress, volumetric strain is another

important deformation variable in the consolidated drained triaxial compression test of coarse-grained materials.

Similarly, the volumetric strain can be divided into elastic strain and plastic strain, i.e.,

$$\varepsilon_{\mathrm{v}} = \varepsilon_{\mathrm{v}}^{\mathrm{e}} + \varepsilon_{\mathrm{v}}^{\mathrm{p}} \tag{17}$$

where ε_{v} is the volumetric strain of coarse-grained materials in the triaxial compression test; $\varepsilon_{\mathrm{v}}^{\mathrm{e}}$ is the elastic volumetric strain; $\varepsilon_{\mathrm{v}}^{\mathrm{p}}$ is the plastic volumetric strain.

According to the theory of elasticity, the relationship between $\varepsilon_{\mathrm{v}}^{\mathrm{e}}$ and $\varepsilon_{\mathrm{a}}^{\mathrm{e}}$ is

$$\varepsilon_{\mathrm{v}}^{\mathrm{e}} = (1-2\nu)\varepsilon_{\mathrm{a}}^{\mathrm{e}} \tag{18}$$

where ν is the Poisson's ratio of coarse-grained material in the undamaged state.

$\varepsilon_{\mathrm{v}}^{\mathrm{p}}$ determines the dilatancy of coarse-grained material, which is closely related to the zigzag shear plane. According to the shear damage mode in Fig. 2, the plastic volumetric strain and axial plastic strain are generated together. Considering the zigzag shear plane, plastic volumetric strain can be expressed as

$$\mathrm{d}\varepsilon_{\mathrm{v}}^{\mathrm{p}} = -K_{\mathrm{x}}\mathrm{d}\varepsilon_{\mathrm{a}}^{\mathrm{p}} \tag{19}$$

where K_{x} is the proportional coefficient of plastic volumetric strain and axial plastic strain, and the relationship between K_{x} and dilatancy angle can be expressed as

$$\sin\psi = \frac{K_{\mathrm{x}}}{2-K_{\mathrm{x}}} \tag{20}$$

For coarse-grained materials, the zigzag shear plane cannot guarantee the continuous linear increase of volumetric strain with the continuous shear damage. In fact, K_{x} will tend to decrease due to the breakage and reorganization of particles, and eventually approach zero when the axial strain increases to a certain extent, that is, the volumetric strain will not change anymore until the deformation develops to the end. The decreasing trend of K_{x} with the increase of plastic strain is close to the law of elastic modulus law in Duncan-Chang model. According to the hyperbolic assumption in Duncan-Chang model, it can be considered that K_{x} and axial plastic strain satisfy the following relationship:

$$K_{\mathrm{x}} = \frac{1}{a(1+b\varepsilon_{\mathrm{a}}^{\mathrm{p}})^2} \tag{21}$$

where both a and b are model constants. By combining Eqs. (19) and (21) and integrating, the relationship between axial plastic strain and plastic volumetric strain can be obtained, as shown in the following equation:

$$\varepsilon_{\mathrm{v}}^{\mathrm{p}} = -\frac{\varepsilon_{\mathrm{a}}^{\mathrm{p}}}{a(1+b\varepsilon_{\mathrm{a}}^{\mathrm{p}})} \tag{22}$$

When Eq.(21) is used to calculate K_{x}, the axial plastic strain and plastic volumetric strain obtained meet the hyperbolic form. Although the Duncan-Chang model assumes that the axial strain and the volumetric strain satisfy the hyperbolic form, it does not distinguish the elastic part and the plastic part, nor does it explain the physical meaning. For loose soil, the deformation is mainly plastic deformation, so the hyperbolic assumption in Duncan-Chang model can be considered as a special case of Eq. (22). K_{x} can also be expressed in other forms. The key is to express the law that the dilatancy decreases with the increase of plastic strain.

By combining Eqs. (17), (18) and (22), the volumetric strain can be expressed as

$$\varepsilon_{\mathrm{v}} = (1-2\nu)\varepsilon_{\mathrm{a}}^{\mathrm{e}} - \frac{\varepsilon_{\mathrm{a}}^{\mathrm{p}}}{a(1+b\varepsilon_{\mathrm{a}}^{\mathrm{p}})} \tag{23}$$

2.5 Stress−strain simulation

According to the *standard for geotechnical testing method* (GB/T50123−2019) [20], in the loading process of triaxial compression test on coarse-grained materials, the loading rate of axial strain should be kept at a fixed value, that is, the deformation servo control.

To further analyze the applicability of the shear damage model, the whole stress−strain process is simulated according to Eqs. (16) and (23).

(1) The state of coarse-grained material after consolidation is regarded as the initial state, and the deviatoric stress is set as $q = \sigma_1 - \sigma_3$. Then the parameters q, ε_1, $\varepsilon_{\mathrm{a}}^{\mathrm{e}}$, $\varepsilon_{\mathrm{a}}^{\mathrm{p}}$, and ε_{v} of stress−strain in the initial state are all 0.

(2) It is assumed that the axial strain increment of each time step is $\mathrm{d}\varepsilon_{\mathrm{a}}$, and the axial elastic strain increment $\mathrm{d}\varepsilon_{ai}^{\mathrm{e}}$ of the step i and the axial plastic strain increment $\mathrm{d}\varepsilon_{a(i-1)}^{\mathrm{p}}$ of the step $i-1$ meet the following relationship, that is, the elastic strain of the next step is controlled according to the plastic strain of the previous step during servo:

$$\mathrm{d}\varepsilon_{\mathrm{a}} = \mathrm{d}\varepsilon_{ai}^{\mathrm{e}} + \mathrm{d}\varepsilon_{a(i-1)}^{\mathrm{p}} \tag{24}$$

Then the deviatoric stress q_i of the step i can be obtained by the following equation:

$$q_i = E\sum \mathrm{d}\varepsilon_{ai}^{\mathrm{e}} \tag{25}$$

(3) T_i can be calculated according to Eq. (16). T_i is actually the part beyond the interface friction. When T_i is less than 0, it indicates that the stress of shear band can be fully contributed by the frictional force, and there will be no loss of interlock force. In the specific calculation, T_i satisfies the following equation:

$$T_i = \begin{cases} q_i \sin\beta\cos\beta - f(q_i\sin^2\beta + \sigma_3), T_{\mathrm{x}} > 0 \\ 0, T_{\mathrm{x}} \leqslant 0 \end{cases} \tag{26}$$

where

$$T_{\mathrm{x}} = q_i \sin\beta\cos\beta - f(q_i\sin^2\beta + \sigma_3) \tag{27}$$

(4) c_i can be calculated according to Eq.(16). As can be seen from Eq.(11), damage factor D is closely related to c_i. Considering that damage is unrecoverable, c_i satisfies the following equation:

$$c_i=\begin{cases}\dfrac{\sum(\mathrm{d}\varepsilon_{\mathrm{a}}-\mathrm{d}\varepsilon^{\mathrm{e}}_{\mathrm{a}(i-1)})}{K}+T_i,\ c_{\mathrm{x}}>c_{(i-1)}\\ c_{(i-1)},c_{\mathrm{x}}\leqslant c_{(i-1)}\end{cases}\tag{28}$$

where

$$c_{\mathrm{x}}=\frac{\sum(\mathrm{d}\varepsilon-\mathrm{d}\varepsilon^{\mathrm{e}}_{\mathrm{a}(i-1)})}{K}+T_i\tag{29}$$

(5) Similarly, the plastic strain increment $\mathrm{d}\varepsilon^{\mathrm{p}}_{ai}$ of the step i can be calculated according to Eq.(16). Considering that plastic strain is unrecoverable, $\mathrm{d}\varepsilon^{\mathrm{p}}_{ai}$ satisfies the following equation:

$$\mathrm{d}\varepsilon^{\mathrm{p}}_{ai}=\begin{cases}T_iK\left\{\dfrac{1}{\exp\left[-\left(\dfrac{c_i}{C_0}\right)^m\right]}-1\right\}-\sum\mathrm{d}\varepsilon^{\mathrm{p}}_{\mathrm{a}(i-1)},\ \mathrm{d}\varepsilon^{\mathrm{p}}_{\mathrm{x}}>0\\ 0,\ \mathrm{d}\varepsilon^{\mathrm{p}}_{\mathrm{x}}<0\end{cases}\tag{30}$$

where

$$\mathrm{d}\varepsilon^{\mathrm{p}}_{\mathrm{x}}=T_iK\left\{\frac{1}{\exp\left[-\left(\dfrac{c_i}{C_0}\right)^m\right]}-1\right\}-\sum\mathrm{d}\varepsilon^{\mathrm{p}}_{\mathrm{a}(i-1)}\tag{31}$$

(6) The volumetric strain increment $\mathrm{d}\varepsilon_{\mathrm{v}i}$ of the step i can be calculated according to Eq. (23).

$$\mathrm{d}\varepsilon_{\mathrm{v}i}=(1-2\nu)\mathrm{d}\varepsilon^{\mathrm{e}}_{ai}+\frac{a\mathrm{d}\varepsilon^{\mathrm{p}}_{ai}}{(a+b\sum\varepsilon^{\mathrm{p}}_{ai})^2}\tag{32}$$

(7) Repeat the steps 1 to 6 until the end of simulation conditions are met.

2.6 Parameter determination based on genetic algorithm

It can be seen from Eqs. (16) and (23) that the model parameters to be determined mainly include E, K, C_0, m, f, β, ν, a, b, etc., and the size of the shear band and the characteristic parameter of the dilatancy are difficult to be directly determined through tests. At the same time, the traditional method of determining parameters based on the stress−strain curve is very complicated, so it is difficult to realize the parameter determination in these complex equations. Based on this, the optimal parameters are determined by genetic algorithm.

The genetic algorithm belongs to the biological evolutionary algorithm. It generates a series of parameter populations by limiting the range of parameter values. In accordance with the principle of 'survival of the fittest', based on the fitness of individuals in the population, the genetic algorithm simulates the selection, crossover, mutation, and other operations of the actual population in nature to generate populations with higher fitness and completes a population evolution. The genetic algorithm achieves the optimization of parameters through continuous iterative evolution until the optimal population individuals with the best fitness are obtained[21]. The process of determining the optimal parameters of the shear damage model based on the genetic algorithm is shown in Fig.4, where the fitness is defined as the error value of the stress−strain curve simulated by the shear model parameters and the actual stress−strain curve. The individual with the smallest error value corresponds to the optimal parameter.

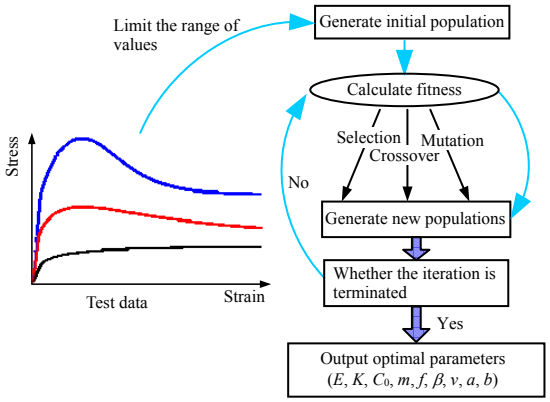

Fig. 4 Schematic graph of genetic algorithm

3 Verification of shear damage model

3.1 Triaxial compression test

According to the *Standard for geotechnical testing method* [20], two groups (#1, #2) of large-scale consolidated drained shear tests were carried out on coarse-grained materials using the ST-1500 electro-hydraulic servo static triaxial tester. The size of the sample was Φ30 cm×60 cm, and the confining pressures were 300, 600, 900 and 1 200 kPa, respectively. The coarse-grained materials used in the two groups of tests were taken from calcareous siltstone in the middle and upper reaches of the Yellow River, with a maximum particle size of 60 mm. The density of the sample in Group #1 was 2.06 g/cm^3 and the porosity of the sample was 21.5%. The density of the sample in Group #2 was 2.08 g/cm^3 and the porosity of the sample was 20.2%. The particle grading curves are shown in Fig. 5.

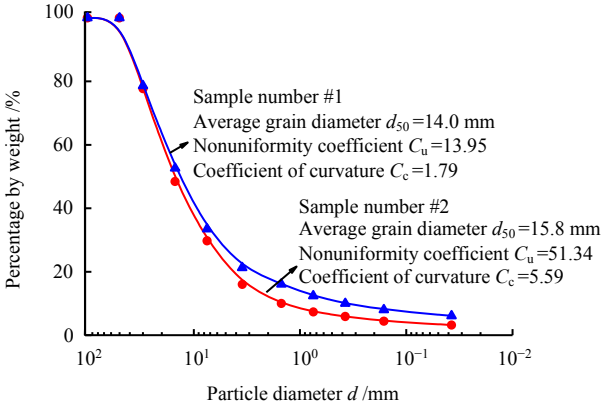

Fig. 5 Particle grading curves of coarse-grained samples in triaxial compression test

The stress−strain curves of the coarse-grained material obtained from the test are shown in Fig.6. The samples in Group #2 contain more coarse particles, and their peak strength and dilatancy are slightly higher than those in Group #1. The softening degree R is defined as the ratio of the stress corresponding to the strain in the last stage to the peak stress. Under different confining pressures, the softening degree of coarse-grained material is shown in Fig.6. One can see from Fig.6 that, under different confining pressures, coarse-grained materials all exhibit certain strain softening characteristics. On the whole, with the increase of confining pressure, strain softening presents a slightly decreasing trend. Meanwhile, there was still some discreteness during the test due to the inability to mix coarse-grained materials completely and evenly. Specifically, the axial strain−volumetric strain curves of the samples in Group #1 under the confining pressures of 600 kPa and 900 kPa partially cross at the later stage of deformation, but the overall evolution of the curves of the samples in Group #2 is basically consistent with the results of previous studies. Some important mechanical characteristics, such as dilatancy and stress−strain curve softening, can be presented in the test curve. With the increase of confining pressure, these two characteristics weaken to a certain extent, and the test results are consistent with the existing research results [8].

3.2 Stress−strain curve simulation

In order to verify the rationality of the shear damage model, the servo process in the triaxial compression test on coarse-grained materials was realized through MATLAB programming based on Eqs. (16) and (23). The damage model parameters of different stress−strain curves were automatically fitted by genetic algorithm, including elastic modulus E, Weibull distribution parameters C_0 and m, the friction parameter of micro-units f, shear failure angle β, Poisson ratio v, a and b related to plastic volumetric strain. The number of populations of genetic algorithm is 50, the probabilities of crossover and mutation are 0.2 and 0.1, respectively, and the number of iterations is 40 000. The damage model parameters of different samples obtained through genetic algorithm fitting are shown in Table 1 and Table 2.

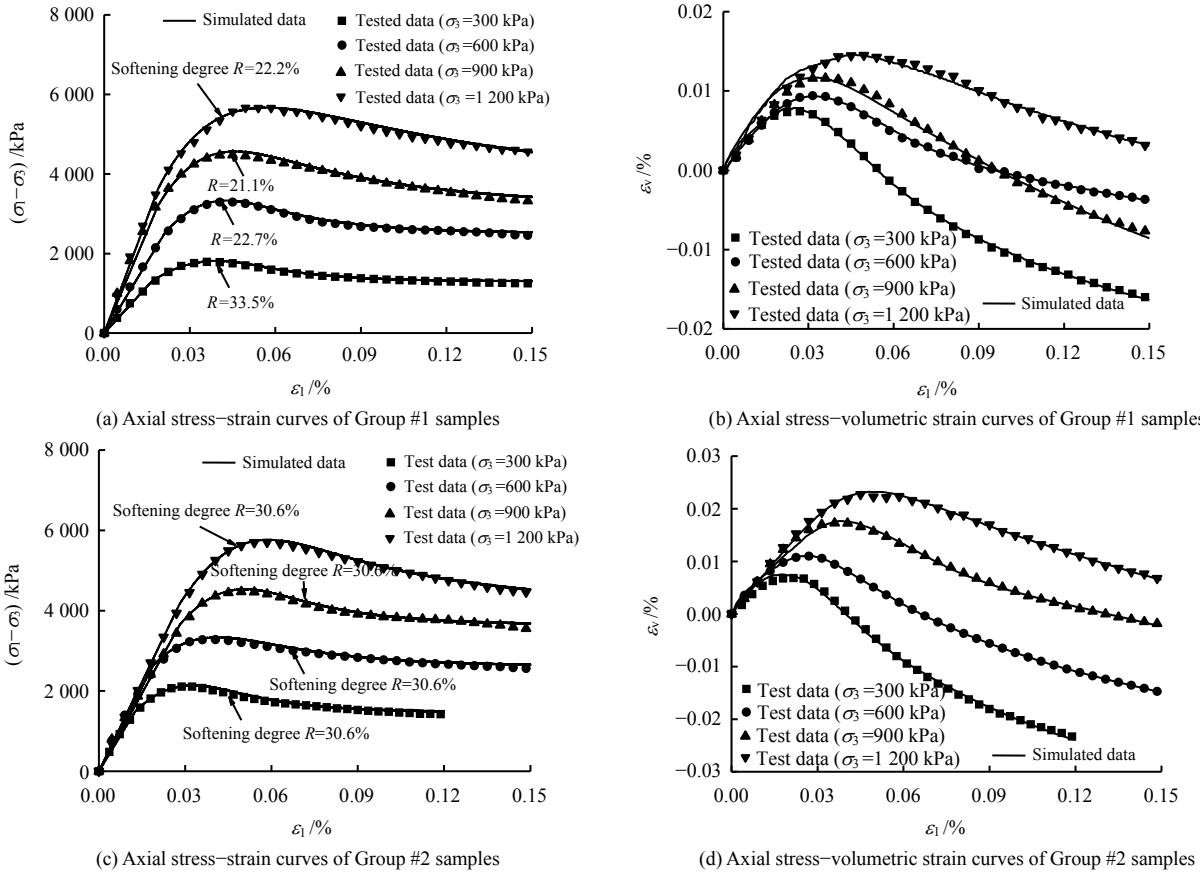

(a) Axial stress−strain curves of Group #1 samples

(b) Axial stress−volumetric strain curves of Group #1 samples

(c) Axial stress−strain curves of Group #2 samples

(d) Axial stress−volumetric strain curves of Group #2 samples

Fig. 6 Comparison of simulated and measured stress−strain values of coarse-grained materials

Table 1 Shear damage model parameters of Group #1 specimens

Confining pressure /kPa	E /MPa	K /10^{-6}	C_0 /kPa	m	f	β /(°)	v	a	b
300	73.6	45.990	316.43	0.836 7	0.913 5	20.60	0.299	2.921	7.295
600	117.6	32.533	492.82	0.849 6	0.890 1	19.59	0.305	4.958	9.117
900	185.0	16.740	986.35	0.676 5	0.770 9	23.24	0.216	5.718	1.731
1 200	202.0	6.918	1 484.74	0.513 8	0.595 1	23.83	0.222	12.785	−

Note: − represents that the weakening of dilatancy with increasing strain is not observed in the axial strain−volume strain curve, and parameter b could not be calculated.

Table 2 Shear damage model parameters of Group #2 specimens

Confining pressure /kPa	E /MPa	K /10^{-6}	C_0/kPa	m	f	β/(°)	v	a	b
300	113.1	46.804	325.74	0.847 1	0.816 4	12.55	0.234	2.000	6.980
600	136.9	32.788	425.82	0.726 1	0.892 6	18.81	0.220	2.711	6.887
900	129.5	23.795	544.66	0.740 7	0.880 7	21.62	0.213	3.531	7.553
1 200	146.7	15.288	1 026.02	0.688 9	0.789 3	22.25	0.182	8.919	−

Note: − represents that the weakening of dilatancy with increasing strain is not observed in the axial strain−volume strain curve, and parameter b could not be calculated.

The optimal parameters of the shear damage model were obtained by genetic algorithm. Through the servo process of the triaxial compression test, the stress−strain relationship was simulated. During the simulation, the axial strain increment was set as 1.5×10^{-4} at each step, and a total of 1 000 steps were simulated. The comparison between simulated values and measured values is shown in Fig.6. Figure 6 shows that the shear damage model can simulate the axial stress−strain curve and axial strain−volumetric strain curve with high accuracy, and the shear damage model does not contain parameters such as peak strength, which means that the peak strength is considered to be a process quantity during loading, rather than a unique parameter.

From the above analysis, it can be found that the derivation process of shear damage model is simple and the physical meaning is clear, which can effectively characterize the mechanism of strain softening and dilatancy for coarse-grained materials in triaxial compression tests.

3.3 Relationship between model parameters and confining pressure

According to Table 1 and Table 2, the confining pressure significantly affects the values of parameters in the shear damage model. With the increase of confining pressure, the elastic modulus increases and the Poisson's ratio shows a decreasing trend. The parameter a related to the volumetric strain represents the shear dilatancy at the initial stage of damage. With the increase of the confining pressure, the parameter a also increases, which corresponds to the weakening of the shear dilatancy according to Eq. (23). Parameter b represents the weakening trend of dilatancy with the increase of plastic strain. As shown in Table 1, the increase of confining pressure can reduce this weakening trend to a certain extent. However, as it involves the strong breakage and reorganization of particles inside the shear band, the variation of parameter b is very complicated, but its overall trend is decreasing. The frictional strength is an important part of the strength of coarse-grained materials. With the increase of confining pressure, the friction coefficient f tends to decrease. The distribution parameter C_0 of cohesion strength of shear micro-units has a positive correlation with the confining pressure, while m is negatively correlated with the confining pressure.

The parameters K and β in the shear damage model represent the size and inclination of the shear band, respectively. The parameter K is an intermediate parameter(see Eq. (16)), which is specifically related to sample size, proportionality coefficient H, shear angle β, and shear stiffness k_s. From the microscopic point of view, the shear stiffness is related to the interfacial contact between particles, and there is large deformation inside the shear band, so it is difficult to establish the theoretical relationship directly through the theory of elasticity. For the sake of analysis, the shear stiffness k_s is assumed to be directly proportional to the elastic modulus E, i.e., $k_s \propto E$; from Eq. (16), we can infer $H \propto \dfrac{EK}{\cos\beta}$. Thus, the magnitude of $\dfrac{EK}{\cos\beta}$ directly corresponds to the size of the shear band itself. The relationships between shear band size, shear band inclination and confining pressure are plotted in Fig. 7.

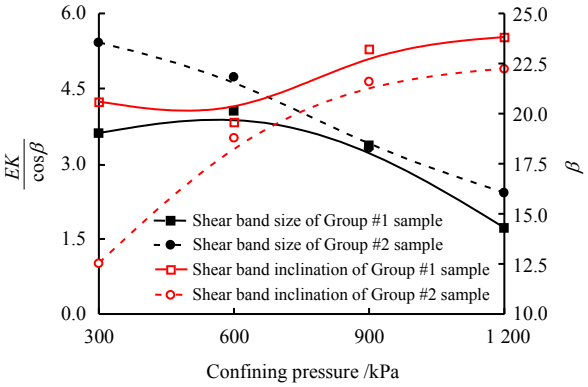

Fig. 7 Relationships between shape parameters of shear band and confining pressure

Figure 7 illustrates that with the increase of confining pressure, the size of shear band tends to decrease and the inclination of shear band tends to increase. It should be noted that the shear band inclination here is mainly the included angle with the direction of the maximum principal stress, that is, the included angle between the shear band and the direction of confining pressure shows a gradually decreasing trend. Desrues et al.[6] systematically summarized the results of consolidated drained triaxial compression tests on loose sand and dense sand under different confining

pressures, and they also revealed that with the increase of confining pressure, the shear band size decreased and the axial inclination increased. Similarly, Gu et al.[4] and Tejchman et al.[5] reproduced this phenomenon from the perspective of numerical simulation using the discrete element method. These results show that the shear damage model cam take into account the characteristics of the shear band itself, which also proves the rationality of the shear damage model, and further reveals the relationship between strain localization characteristics and confining pressure.

3.4 Meso-strength composition

The established shear damage mechanical model can accurately simulate the stress−strain curve of coarse-grained materials in triaxial compression test. From the point of view of strain localization, this study construct a shear damage mechanical model with wide applicability for strain softening characteristics.

For the stress−strain curve of strain softening, the cohesion of the shear band of coarse-grained materials in the shear damage model is mainly related to the interlock force between particles. Particle breakage and particle reorganization correspond to the gradual loss of interlock force. As the parts with weak interlock force are gradually damaged, the parts with strong interlock force need to bear more shear stress gradually. This corresponds to the fact that plastic deformation begins to occur in the stress−strain curve. At this moment, the shear stress contributed by the whole shear band of the sample cam continue to increase. With the continuous increase of shear stress, the part with strong interlock force also begins to show damage, and the whole shear band of the sample will not be able to bear more shear stress. As a result, the strain softening characteristic appears, that is, the strength reches the peak when the shear stress $\Delta\tau$ contributed by the whole shear band of the sample reaches its peak. By combining Eqs. (9) and (11), the shear stress contributed by the sample as a whole can be expressed as follows:

$$c\exp\left[-\left(\frac{c}{C_0}\right)^m\right]=\Delta\tau \tag{33}$$

Taking the derivative of Eq. (33) yields the extreme value. When $c=C_0(\frac{1}{m})^{\frac{1}{m}}$, $\Delta\tau$ reached the peak. The specific equation is as follows:

$$\Delta\tau_{\max}=C_0\left(\frac{1}{m}\right)^{\frac{1}{m}}\exp\left(-\frac{1}{m}\right) \tag{34}$$

By combining Eqs.(2) and (34), the peak strength $(\sigma_1-\sigma_3)_{\mathrm{p}}$ can be obtained as follows:

$$(\sigma_1-\sigma_3)_{\mathrm{p}}=\frac{f\sigma_3+C_0\left(\frac{1}{m}\right)^{\frac{1}{m}}\exp\left(-\frac{1}{m}\right)}{\sin\beta(\cos\beta-f\sin\beta)} \tag{35}$$

When the damage variable D=1, this means that the sample enters a stable plastic flow state, and the final residual strength $(\sigma_1-\sigma_3)_{\mathrm{r}}$ can be expressed as follows:

$$(\sigma_1-\sigma_3)_{\mathrm{r}}=\frac{f\sigma_3}{\sin\beta(\cos\beta-f\sin\beta)} \tag{36}$$

Based on the parameters listed in Table 1 and Table 2, the peak strength, and the residual strength of the samples in Group #1 and Group #2 under different confining pressures were computed according to Eqs. (35) and (36), respectively. The actual peak strength, calculated peak strength and residual strength are plotted in Fig. 8. During the triaxial compression test on coarse-grained materials, a sufficiently large strain is required to achieve residual strength, so the actual residual strength is here no longer analyzed.

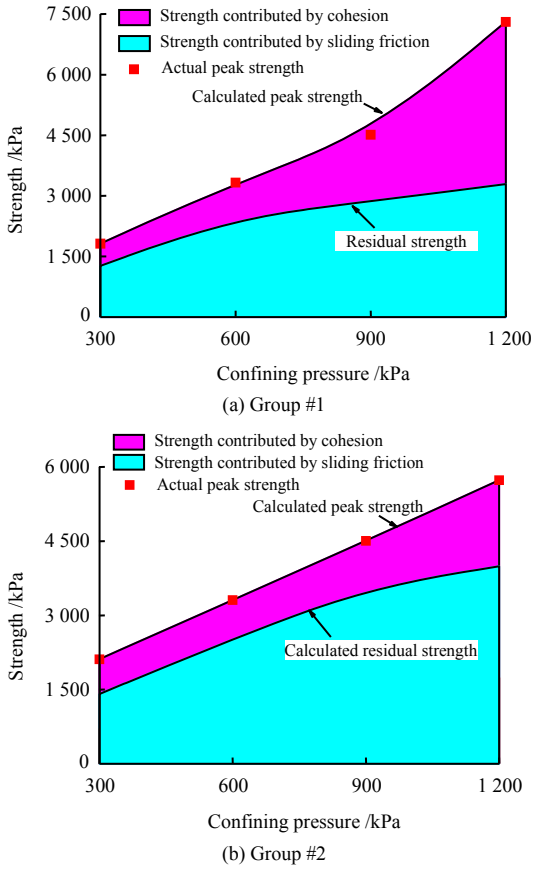

Fig. 8 Peak strength composition of specimens under different confining pressures

It can be observed from Fig. 8 that with the increase of confining pressure, the proportion of the strength contributed by the friction of samples decreases, while the proportion of the strength contributed by the cohesion of samples increases. Lee et al.[22] qualitatively drew the strength composition considering particle breakage by conducting consolidated drained triaxial compression tests on sand, as shown in Fig.9 (a). From the perspective of energy, the external force does negative work during dilation, and its contribution to

cohesion is positive, while during contraction, the contribution of external force to cohesion is negative[22]. Figure 9(a) shows that the cohesion in the shear damage model includes dilatancy (shear contraction), particle breakage and reorganization. In the damage process of coarse-grained materials, the dilatancy prevailed. Considering that the friction coefficient of sliding friction showed a nonlinear decreasing trend, Fig.9(a) was modified to Fig.9(b) to describe the strength composition of coarse-grained materials in combination with the test results in this study. It is noted that the nonlinear characteristics of sliding friction conform to the generalized friction law [23].

With the increase of confining pressure, coarse-grained materials become denser. In the process of failure, the particles inside the shear band are more likely to be broken. Therefore, in general, the contribution of cohesion tends to increase with the confining pressure, while the proportion of strength contributed by sliding friction decreases to a certain extent.

From Eq.(35), it is found that the peak strength of coarse-grained material in triaxial compression test does not contain elastic parameters, that is, the strength of coarse-grained material is mainly associated to the contact characteristics of particle interface, the particle strength itself and the particle shape. The numerical simulation based on particle flow code also reveals that the peak strength is not affected by the elastic parameters of particles [24].

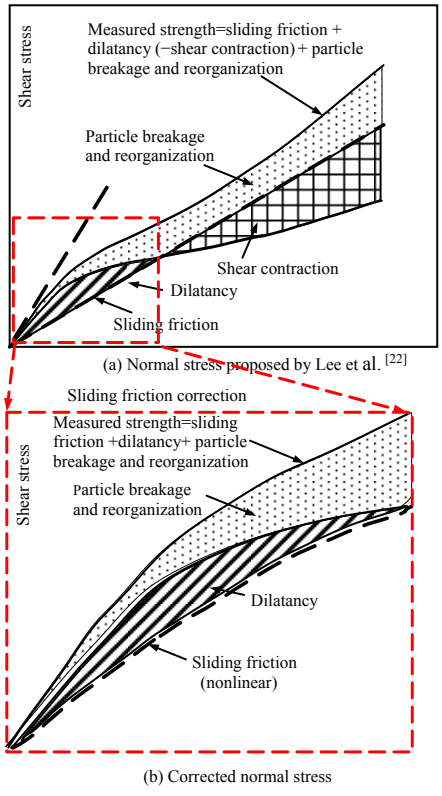

Fig. 9 Schematic diagram of strength composition of coarse-grained materials

4 Influence of cohesion distribution parameters

In order to further analyze the influence of cohesion distribution parameters C_0 and m on the deformation characteristics of coarse-grained materials, the samples under the confining pressure of 1 200 kPa in Group #2 were taken as the research object. The parameter m was set at 0.4, 0.6, 1.0 and 2.0, respectively, while other cohesion distribution parameters remained unchanged. The cohesion probability distribution function and the axial stress−strain relationship are plotted as shown in Figs. 10 (a) and 11 (a). When C_0 was set at 100, 500, 1 000 and 2 000 kPa, respectively, the corresponding cohesion probability distribution function and axial stress−strain relationship are presented in Figs.10 (b) and 11 (b).

In the Weibull distribution function, m is the shape parameter and C_0 is the scale parameter. It can be seen from Figs.10 and 11 that with the increase of m, the distribution of cohesion is relatively concentrated, which is consistent with that the in the stress−strain curve, there is an obvious shift from ductile failure to brittle failure, but the change of peak value is relatively not obvious. Therefore, m mainly reflects the concentration of cohesion distribution. For geotechnical materials, m can characterize the internal homogeneity of the material to a certain extent. For soil materials, due to a large number of internal pores, in the cohesion distribution of shear band, there are more units with small cohesion. The stress−strain curve shows more characteristics of strain hardening, and the plastic deformation is obvious. For homogeneous rock materials, the cohesion distribution is relatively concentrated, and the stress−strain curve shows prominent strain softening characteristics. Thus, m can be used as an indicator of strain hardening and strain softening to a certain extent. As can be seen from Fig.10, the larger the value of C_0 is, the greater the proportion of large cohesion in the cohesion distribution is, and the peak strength changes significantly in the stress−strain curve. Consequently, C_0 is an important index affecting the overall cohesion.

For the samples in Group #1 and Group #2, with the increase of confining pressure, the contact force between particles increases, corresponding to the enhancement of the interlock force effect. C_0 hence increases significantly with the increase of confining pressure. In terms of parameter m, with the increase of confining pressure, the interlock force between particles increases. Due to the small contact area between particles, the enhancement of the interlock force between particles is more noticeable for the original strong contact part, while the weak contact part has a small increase due to the limited stress it bore, resulting in a more dispersed internal cohesion distribution and a decreasing trend of m.

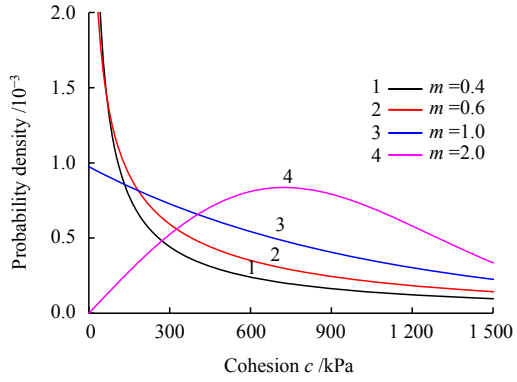

(a) Variation of m

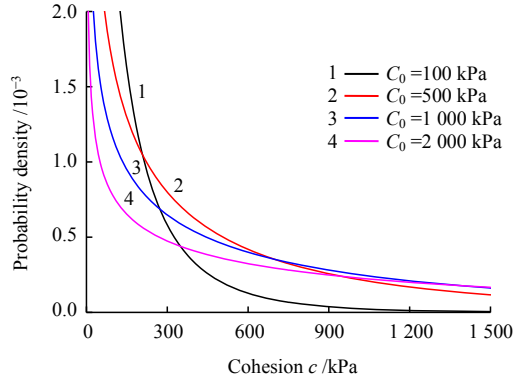

(b) Variation of C_0

Fig. 10 Effects of parameter variation on probability density function of cohesion

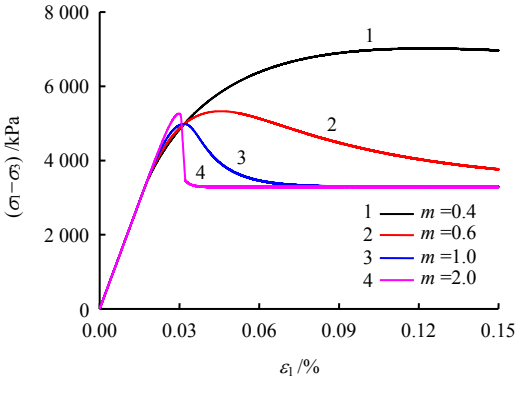

(a) Variation of m

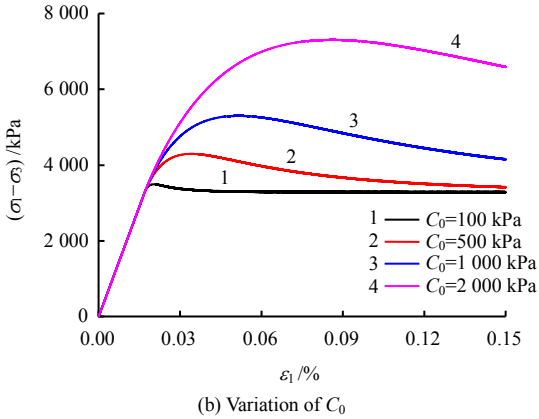

(b) Variation of C_0

Fig. 11 Effects of parameter variation on stress−strain curves

Through the discussion of parameters C_0 and m, it can be found that the shear damage model can effectively characterize the deformation and failure characteristics of coarse-grained materials, and also has the ability to simulate strain hardening and strain softening. It has a wide range of applicability, and effectively reveals the influencing mechanism of the parameters inside the shear band on the overall macroscopic deformation of the sample.

5 Conclusions

Considering the strain localization characteristics of coarse-grained materials, a shear damage mechanical model of coarse-grained materials was established based on inclusion theory, strain equivalence principle and Weibull distribution. The physical meaning of the parameters in the damage model is clear, and the derivation process is simple. At the same time, this proposed model can better simulate the strength and deformation characteristics of coarse-grained materials, and effectively reveal the influencing mechanism of the deformation inside the shear band of coarse-grained materials considering the strain localization characteristics on the overall macroscopic deformation of the sample. The following conclusions can be drawn from the present study:

(1) The shear damage model established in this study considering strain localization characteristics can accurately simulate the stress−strain curve characteristics of coarse-grained materials under different confining pressures, and it can also simulate the characteristics of strain hardening, strain softening and dilatancy, which has universal applicability.

(2) The shear damage model can well present the characteristics of dilatancy weakening. Based on the dilatancy mechanism, the axial plastic strain and the plastic volumetric strain show a nonlinear relationship.

(3) With the increase of confining pressure, the shear band size revealed by the model tends to increase, and the included angle between the shear band and the maximum principal stress direction tends to decrease, which is basically consistent with the existing research results.

(4) In the cohesion distribution function, the parameter C_0 is positively correlated with the confining pressure. The larger the value of C_0 is, the greater the proportion of large cohesion in the cohesion distribution is. C_0 is an important index affecting the overall cohesion. Parameter m is negatively correlated with confining pressure. Parameter m mainly reflects the concentration of cohesion distribution, and it can be used as an indicator of strain hardening and strain softening to some extent.

(5) The strength composition of coarse-grained materials is mainly determined by cohesion and frictional

strength. The breakage and reorganization of particles are important components of cohesion. With the increase of confining pressure, the proportion of strength contributed by the breakage and reorganization of particles tended to increase.

References

[1] LIU Si-hong, SHAO Dong-chen, SHEN Chao-min, et al. Microstructure-based elastoplastic constitutive model for coarse-grained materials[J]. Chinese Journal of Geotechnical Engineering, 2017, 39(11): 777−783.

[2] WANG H L, CUI Y J, LAMAS-LOPEZ F, et al. Investigation on the mechanical behavior of track-bed materials at various contents of coarse grains[J]. Construction and Building Materials, 2018, 164: 228−237.

[3] JIANG Jing-shan, CHENG Zhan-lin, ZUO Yong-zhen, et al. Effects of stress state on mechanical properties of coarse granular material using large-scale true triaxial tests[J]. Rock and Soil Mechanics, 2017, 38(Suppl. 2): 131−137.

[4] GU X, HUANG M, QIAN J. Discrete element modeling of shear band in granular materials[J]. Theoretical and Applied Fracture Mechanics, 2014, 72: 37−49.

[5] TEJCHMAN J, GÓRSKI J, EINAV I. Effect of grain crushing on shear localization in granular bodies during plane strain compression[J]. International Journal for Numerical and Analytical Methods in Geomechanics, 2012, 36(18): 1909−1931.

[6] DESRUES J, VIGGIANI G. Strain localization in sand: an overview of the experimental results obtained in Grenoble using stereo photogrammetry[J]. International Journal for Numerical and Analytical Methods in Geomechanics, 2004, 28(4): 279−321.

[7] WANG Yi-wei, LIU Run, SUN Ruo-han, et al. Macroscopic and mesoscopic correlation of granular materials based on rolling resistance linear contact model[J]. Rock and Soil Mechanics, 2022, 43(4): 945−956.

[8] JIA Yu-feng, CHI Shi-chun, LIN Gao. Constitutive model for coarse granular aggregates incorporating particle breakage[J]. Rock and Soil Mechanics, 2009, 30(11): 3261−3266.

[9] LIU M, GAO Y. Constitutive modeling of coarse-grained materials incorporating the effect of particle breakage on critical state behavior in a framework of generalized plasticity[J]. International Journal of Geomechanics, 2017, 17(5): 04016113.

[10] HOU F, LAI Y, LIU E, et al. A creep constitutive model for frozen soils with different contents of coarse grains[J]. Cold Regions Science and Technology, 2018, 145: 119−126.

[11] LING X, TIAN S, TANG L, et al. A damage-softening and dilatancy prediction model of coarse-grained materials considering freeze–thaw effects[J]. Transportation Geotechnics, 2020, 22: 100307.

[12] BRADY B T. Theory of earthquakes[J]. Pure and Applied Geophysics, 1974, 112(4): 701−725.

[13] LIU Te-hong, LIN Tian-jian. Design theory and construction practice of soft rock engineering[M]. Beijing: China Architecture & Building Press, 2001.

[14] MA G, ZHOU W, CHANG X, et al. Formation of shear bands in crushable and irregularly shaped granular materials and the associated microstructural evolution[J]. Powder Technology, 2016, 301: 118−130.

[15] DESRUES J, CHAMBON R, MOKNI M, et al. Void ratio evolution inside shear bands in triaxial sand specimens studied by computed tomography[J]. Géotechnique, 1996, 46(3): 529−546.

[16] ROWE P W. The stress-dilatancy relation for static equilibrium of an assembly of particles in contact[J]. Proceedings of the Royal Society of London (Series A): Mathematical and Physical Sciences, 1962, 269(1339): 500−527.

[17] REN F, HE J, ZHANG F, et al. Numerical investigation of the influence of non-uniform factors on the monotonic/cyclic behaviour of coarse-grained soil[J]. Computers and Geotechnics, 2018, 103: 115−137.

[18] LEMAITRE J. How to use damage mechanics[J]. Nuclear Engineering and Design, 1984, 80(2): 233−245.

[19] WEIHULL W. A statistical distribution function of wide applicability[J]. Journal of Applied Mechanics, 1951, 18(3): 290−293.

[20] Ministry of Water Resources of the People's Republic of China. GB/T50123 — 2019 Standard for geotechnical testing method[S]. Beijing: China Planning Press, 2019.

[21] HOLLAND J H. Outline for a logical theory of adaptive systems[J]. Journal of the ACM, 1962, 9(3): 297−314.

[22] LEE K L, SEED H B. Drained strength characteristics of sands[J]. Journal of the Soil Mechanics and Foundations Division, 1993(6): 117−141.

[23] HUANG Ping, LAI Tian-mao. Friction model based on real contact area[J]. Journal of South China University of Technology (Natural Science Edition), 2012, 40(10): 109−114.

[24] CHANG Zai. Theoretical and numerical research on granular mechanics of soils[D]. Beijing: Tsinghua University, 2008.